Multifunctional Coordination Compounds Based on Lanthanide Ions and 5-Bromonicotinic Acid. Magnetic, Luminescence and Anti-Cancer Properties

Cristina Ruiz,[a] Antonio A. García-Valdivia,[a] Belén Fernández,[b] Javier Cepeda,[c] Itziar Oyarzabal,[c] Elisa Abas,[d] Mariano Laguna,[d] Jose Angel García,[e] Ignacio Fernández,[f] Eider San Sebastián[c,*] and Antonio Rodríguez-Diéguez [a,*]

- Single crystal X-ray diffraction data for compounds **1-4**
- Continuous shape measurements for compounds **1-4**
- Additional description of structural and packing features of compounds **1-4**
- Magnetic properties
- Additional information on photoluminescence properties of compounds **1-4**

Single Crystal X-ray Diffraction

Table S1. Crystallographic data and refinement details of compounds **1-4**

Compound	**1**	**2**	**3**	**4**
Chem. form.	$C_{18}H_{17}Br_3DyN_3O_{10}$	$C_{24}H_{19}Br_4N_4O_{11}Tb$	$C_{24}H_{19}Br_4N_4O_{11}Yb$	$C_{18}H_{17}Br_3N_3NdO_{10}$
CCDC	1882984	1882985	1882986	1882987
Form. weight	837,57	1017,99	1032,11	819,31
Cryst. system	Triclinic	Monoclinic	Monoclinic	Triclinic
Space group	*P*-1	*P*2/c	*P*2/c	*P*-1
a (Å)	7.4580(4)	11.686(5)	11.686(5)	10.1630(5)
b (Å)	10.6630(6)	15.970(5)	15.970(5)	11.5260(6)
c (Å)	15.6770(7)	16.742(5)	16.742(4)	11.6110(6)
α (º)	82.162(2)	90.000(5)	90.000(5)	88.319(2)
β (º)	87.933(2)	90.246(5)	90.246(5)	85.525(2)
γ (º)	72.310(2)	90.000(5)	90.000(5)	69.254(2)
V (Å^3)	1176.64(11)	3124.45(19)	3132.45(21)	1268.03(11)
Z	2	4	4	2
GOF [a]	1.024	1.030	1.023	1.017
R_{int}	0.0787	0.1106	0.1487	0.0721
R_1[b] / wR^2[c] [I>2σ(I)]	0.0275	0.0355	0.0558	0.0278
R_1[b] / wR^2[c] (all data)	0.0446	0.0613	0.1166	0.0431

[a] $S = [\sum w(F_0^2 - F_c^2)^2 / (N_{obs} - N_{param})]^{1/2}$

[b] $R_1 = \sum||F_0|-|F_c|| / \sum|F_0|$ [c] $wR_2 = [\sum w(F_0^2 - F_c^2)^2 / \sum wF_0^2]^{1/2}$

$w = 1/[\sigma^2(F_0^2) + (aP)^2 + bP]$ where $P = (\max(F_0^2,0) + 2Fc^2)/3$

Table S2. Selected bond distances (Å) in compounds **1-4**

1		**2**		**3**		**4**	
Dy(1)-O(1)	2.280 (2)	Tb(1)-O(1)	2.517(3)	Yb(1)-O(1)	2.494(4)	Nd(1)-O(1)	2.386(2)
Dy(1)-O(2)	2.334 (2)	Tb(1)-O(2)	2.456(3)	Yb(1)-O(2)	2.411(4)	Nd(1)-O(4)	2.507(3)
Dy(1)-O(3)	2.515 (2)	Tb(1)-O(3)	2.456(3)	Yb(1)-O(3)	2.411(4)	Nd(1)-O(6)	2.407(2)
Dy(1)-O(4)	2.373 (2)	Tb(1)-O(4)	2.517(3)	Yb(1)-O(4)	2.494(4)	Nd(1)-O(7)	2.445(2)
Dy(1)-O(5)	2.328 (2)	Tb(1)-O(5)	2.274(3)	Yb(1)-O(5)	2.222(4)	Nd(1)-O(8)	2.476(3)
Dy(1)-O(6)	2.381 (3)	Tb(1)-O(6)	2.274(3)	Yb(1)-O(6)	2.222(4)	Nd(1)-O(9)	2.518(2)
Dy(1)-O(7)	2.364 (3)	Tb(1)-O(7)	2.317(3)	Yb(1)-O(7)	2.267(5)		
Dy(1)-O(8)	2.401 (3)	Tb(1)-O(8)	2.317(3)	Yb(1)-O(8)	2.267(5)		
		Tb(2)-O(9)	2.382(3)	Yb(2)-O(9)	2.340(5)		
		Tb(2)-O10	2.518(3)	Yb(2)-O10	2.463(5)		
		Tb(2)-O11	2.518(3)	Yb(2)-O11	2.463(5)		
		Tb(2)-O12	2.382(3)	Yb(2)-O12	2.340(5)		
		Tb(2)-O13	2.334(3)	Yb(2)-O13	2.290(5)		
		Tb(2)-O14	2.288(3)	Yb(2)-O14	2.245(4)		
		Tb(2)-O15	2.288(3)	Yb(2)-O15	2.290(5)		
		Tb(2)-O16	2.334(3)	Yb(2)-O16	2.245(4)		

*Continuous shape measurementsfor compounds **1-4***

Table S3. Continuous Shape Measurements for compound **1**.

OP-8	D8h	33.634	Octagon
HPY-8	C7v	24.161	Heptagonal pyramid
HBPY-8	D6h	16.053	Hexagonal bipyramid
CU-8	Oh	11.780	Cube
SAPR-8	D4d	3.310	Square antiprism
TDD-8	**D2d**	**1.258**	**Triangular dodecahedron**
JGBF-8	D2d	12.545	Johnson gyrobifastigium
JETBPY-8	D3h	29.152	Johnson elongated triangular bipyramid
JBTPR-8	C2v	3.428	Biaugmented trigonal prism J50
BTPR-8	C2v	2.840	Biaugmented trigonal prism
JSD-8	D2d	3.280	Snub diphenoid J84
TT-8	Td	12.369	Triakis tetrahedron
ETBPY-8	D3h	24.273	Elongated trigonal bipyramid

Tabla S4. Continuous Shape Measurements for compound **2**.

		Tb1	**Tb2**	
OP-8	D8h	29.87103	33.35908	Octagon
HPY-8	C7v	23.87768	20.78742	Heptagonal pyramid

HBPY-8	D6h	12.62887	17.37903	Hexagonal bipyramid
CU-8	Oh	11.50032	11.35744	Cube
SAPR-8	D4d	5.12819	**2.11891**	**Square antiprism**
TDD-8	D2d	3.15688	2.41183	Triangular dodecahedron
JGBF-8	D2d	9.68011	14.84873	Johnson gyrobifastigium
JETBPY-8	D3h	24.42354	28.54568	Johnson elongated triangular bipyramid
JBTPR-8	C2v	4.10154	3.36185	Biaugmented trigonal prism J50
BTPR-8	C2v	3.87065	2.99195	Biaugmented trigonal prism
JSD-8	**D2d**	**2.69732**	4.78272	**Snub diphenoid J84**
TT-8	Td	12.32897	11.89917	Triakis tetrahedron
ETBPY-8	D3h	22.26482	24.09449	Elongated trigonal bipyramid

Tabla S5.*Continuous Shape Measurements for compound **3.***

		Yb1	**Yb2**	
OP-8	D8h	30.03056	32.93346	Octagon
HPY-8	C7v	24.05127	21.19139	Heptagonal pyramid
HBPY-8	D6h	12.92112	16.95599	Hexagonal bipyramid
CU-8	Oh	11.73851	11.13868	Cube
SAPR-8	D4d	5.08143	1.98888	Square antiprism
TDD-8	**D2d**	3.02096	**2.21428**	**Triangular dodecahedron – Yb2**
JGBF-8	D2d	9.58468	14.49641	Johnson gyrobifastigium
JETBPY-8	D3h	24.02648	28.52512	Johnson elongated triangular bipyramid
JBTPR-8	C2v	3.75836	3.16896	Biaugmented trigonal prism J50
BTPR-8	C2v	3.72631	2.81115	Biaugmented trigonal prism
JSD-8	**D2d**	**2.42629**	4.48468	**Snub diphenoid J84 – Yb1**
TT-8	Td	12.56464	11.87074	Triakis tetrahedron
ETBPY-8	D3h	22.07686	24.28132	Elongated trigonal bipyramid

Tabla S6. Continuous Shape Measurements for compound **4**.

OP-8	D8h	31.74487	Octagon
HPY-8	C7v	24.76168	Heptagonal pyramid

HBPY-8	D6h	16.84210	Hexagonal bipyramid
CU-8	Oh	10.80655	Cube
SAPR-8	D4d	2.86138	Square antiprism
TDD-8	D2d	0.76376	Triangular dodecahedron
JGBF-8	D2d	12.76224	Johnson gyrobifastigium
JETBPY-8	D3h	28.58916	Johnson elongated triangular bipyramid
JBTPR-8	C2v	2.03246	Biaugmented trigonal prism J50
BTPR-8	**C2v**	**1.34490**	**Biaugmented trigonal prism**
JSD-8	D2d	2.61602	Snub diphenoid J84
TT-8	Td	11.35385	Triakis tetrahedron
ETBPY-8	D3h	24.49616	Elongated trigonal bipyramid

Additional description of structural and packing features of compounds 1-4

Description of **1**

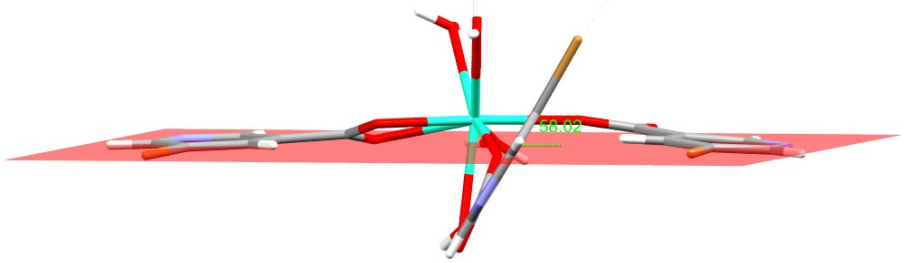

Figure S1. Representation of a monomer of **1**. The oxygen atoms of the four coordinated water molecules are nearly co-planer, whereas the plane containing the aromatic ring of the bidentate nicotinate ligand and one of the monodentated ligands, deviates substantially from being perpendicular to the plane generated by the aromatic ring of the second monodentated ligand (dihedral angle 58.02º). All Dy-O distances are in the range of 2.280(2)-2.515(2) Å (Table S2).

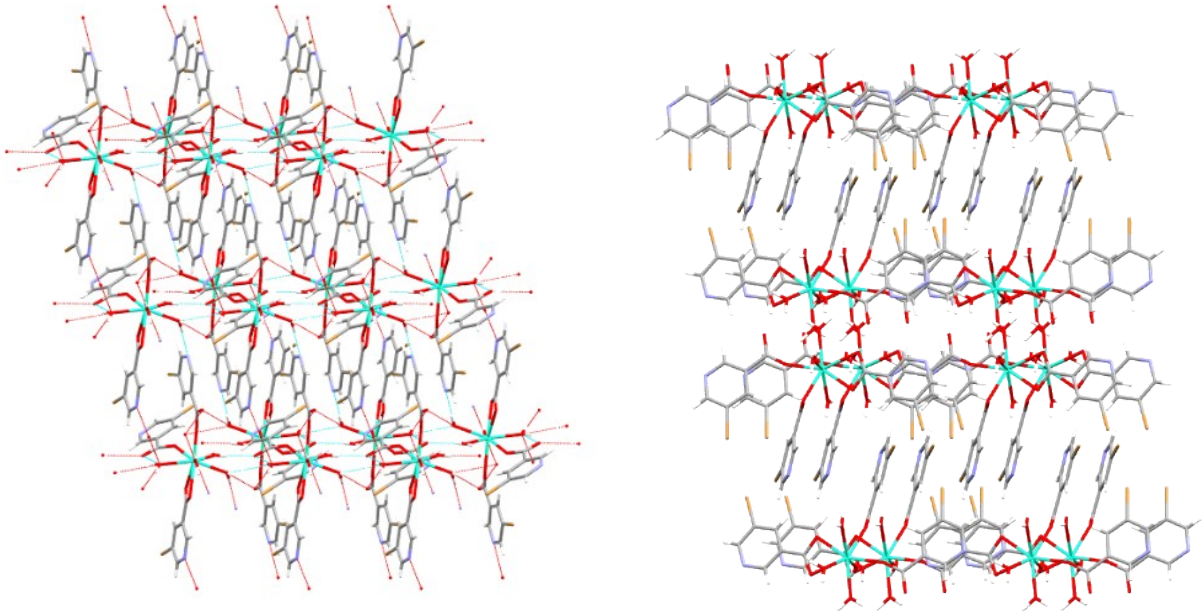

Figure S2. Left: A complex hydrogen-bond network along the **a** axis (primarily) links a central monomer of **1** to seven surrounding copies, with H-bond distances in the usual range of 2.654-3.033Å, except that distance is particularly short in the case of the O2A (carboxylate)-O2W (water molecule), with a value of 2.654 Å. Center: Perspective view of the packing of compound **1**along the *a* axis. Briefly, in addition to the multiple intermolecular H-bonds established between the coordination water molecules of **1** and the surroundingmonomers, the nicotinic N-atom of one monodentated (N1B) as well as the bidentated (N1C) copies of 5-BrNic, and the free carboxylic oxygen atom of both monodentated 5-BrNic ligands (O2A and O2B), stabilize the crystal packing of **1**. Right: Perspective view of the packing of compound **1** along the *b* axis. The packing of 1 is stabilized by π-π stacking interactions established between the aromatic pyridine rings of adjacent monomers. Colour code: Dysprosium, green; oxygen, red; nitrogen blue; carbon, grey; bromine, brown; hydrogen, white.

Description of **2** and **3.**

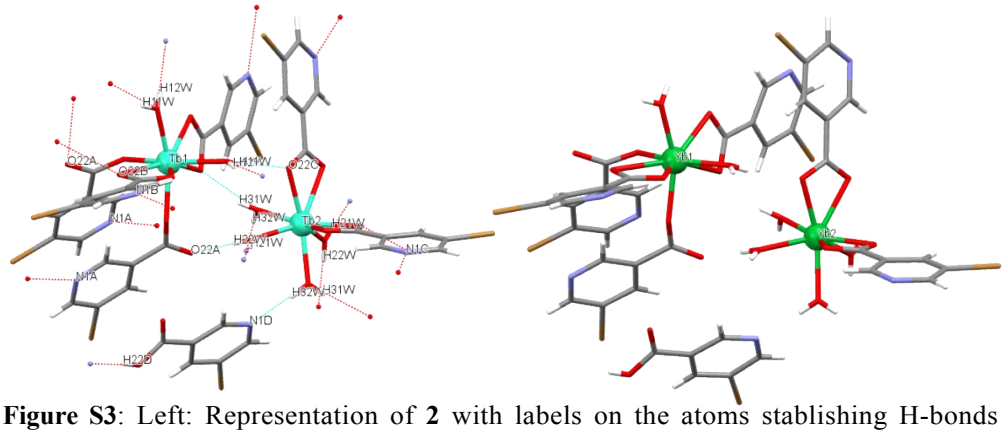

Figure S3: Left: Representation of **2** with labels on the atoms stablishing H-bonds with surrounding units. A complex 3D hydrogen-bond network links Tb1 and Tb2 units, as well as the crystallization ligand, to each other multiple surrounding copies, Both Tb1 and Tb2 units show a TbO_8nearly ideal rectangular antiprism environment, derived from the coordination of: two perpendicular 5-BrNic ligands bound to Tb1 in a bidentate fashion via oxygens O1/O2 and O3/O4, two copies of monodentated ligands (O5 and O6) parallel to each other in the *b* axis, and two water molecules. All Tb-O distances are in the usual 2.274(3)-2.517(3) Å (Table S2). The second Tb(III) unit (Tb2), shows a TbO_8 environment, where the cations coordinates to four water molecules via oxygens (O13, O14, O15 and O16), and two chelate bidentated ligands (O9/O10 and O11 y O12) forming a nearly ideal rectangular antiprism. The third unit consists of a protonated 5-HBrNic crystallization ligand. The packing of the structure reveals a unit cell containing 4 $Tb(5\text{-}BrNic)_4(H_2O)_2$ (**Tb1**) units, two $Tb(5\text{-}BrNic)_2(H_2O)_4$ units and two copies of a 5-HBrNic crystallization ligand. Right: Representation of **3.** The same type of description applies to compound **3**, except that Ln(III)-O distances in **2** are larger than in **3** (see Table S2), which is consistent with the larger nuclear charge of the former.

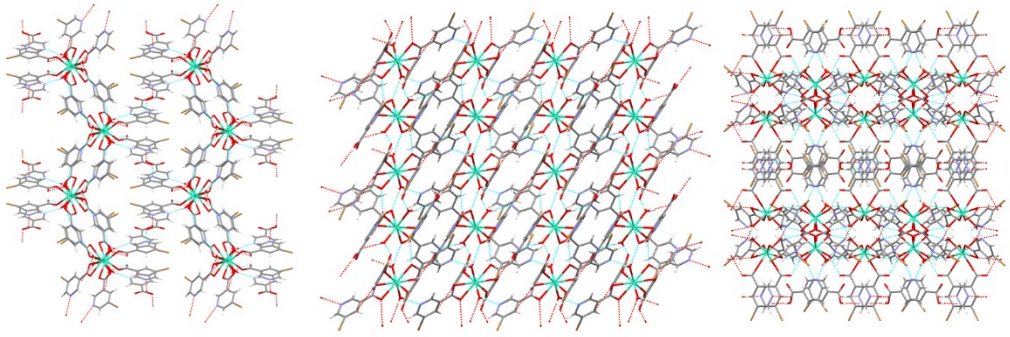

Figure S4. Perspective view of the packing of compounds**2**and **3**along the*a* (left), *b* (centre) and *c* (right) axes.

Description of **4.**

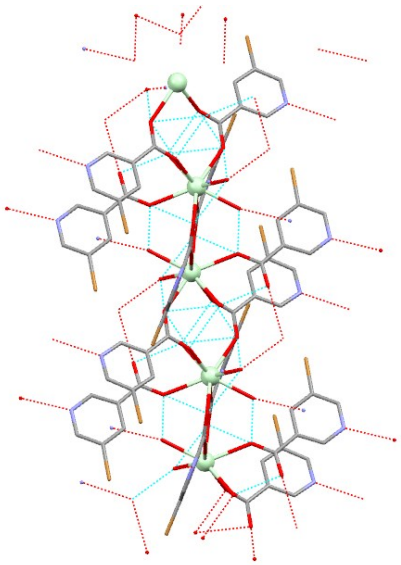

Figure S5. Representation of the H-bond network stablished by a linear chain of **4** along the *b* axis.

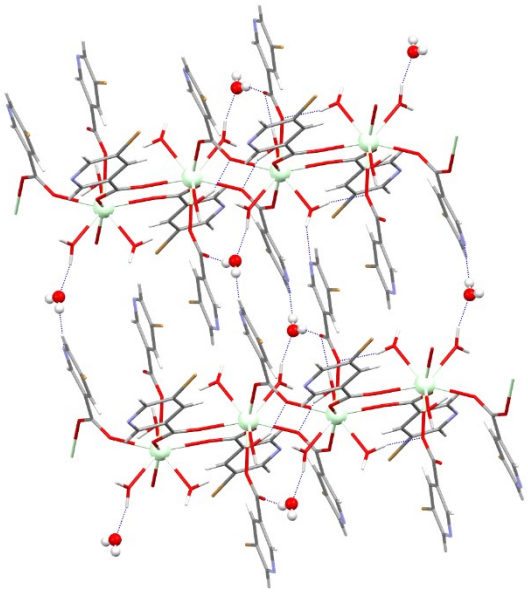

Figure S6. Elongation of a linear chain of **4** along the *a* axis packed through a complex network of H-bonds. Colour code: Neodynium, green; oxygen, red; nitrogen blue; carbon, black; hydrogen, white.

Dc magnetic properties of compounds 1-4

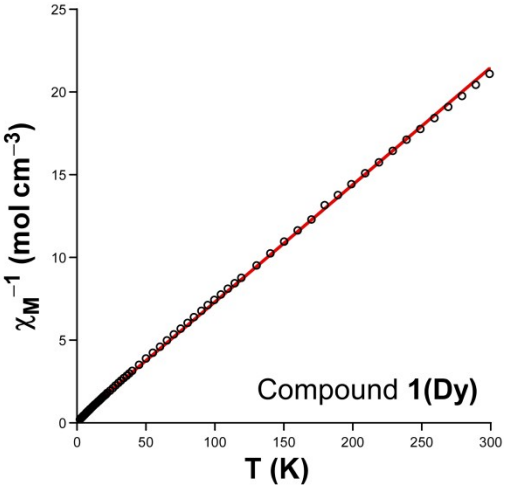

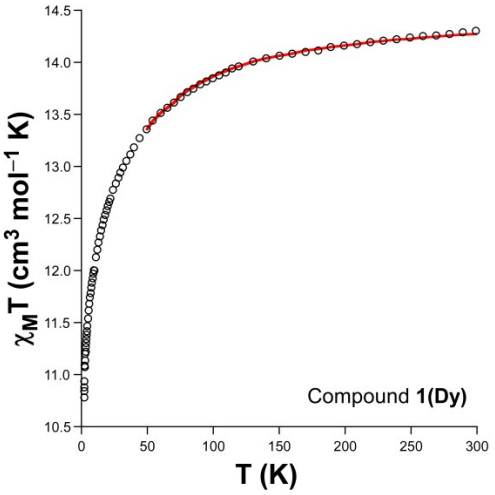

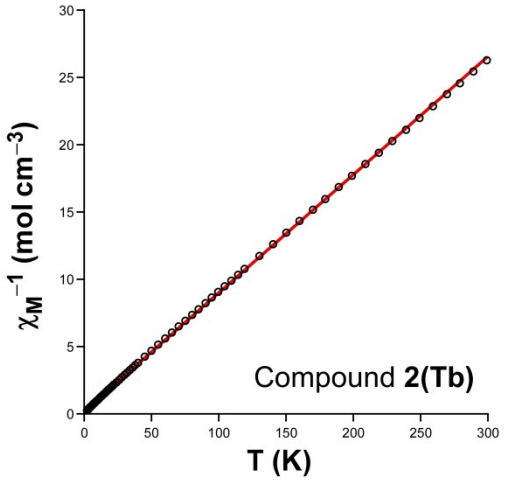

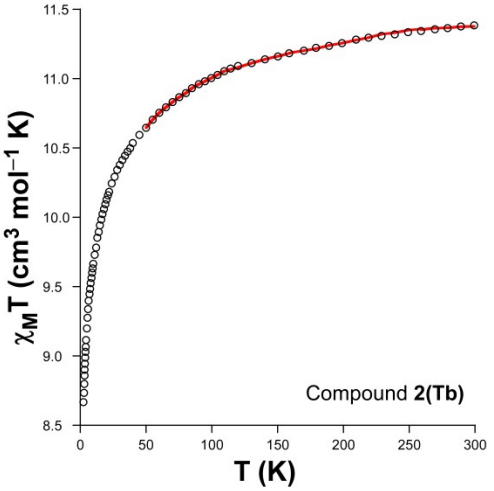

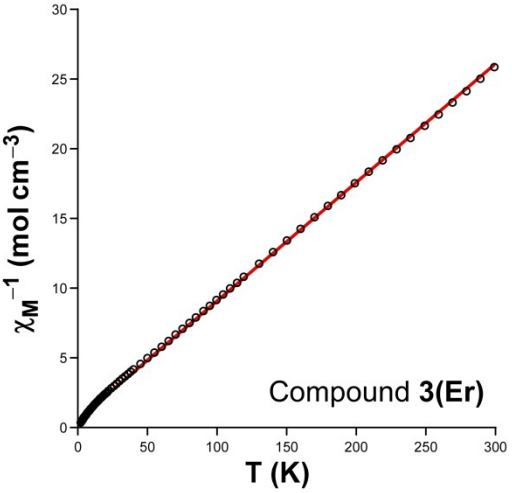

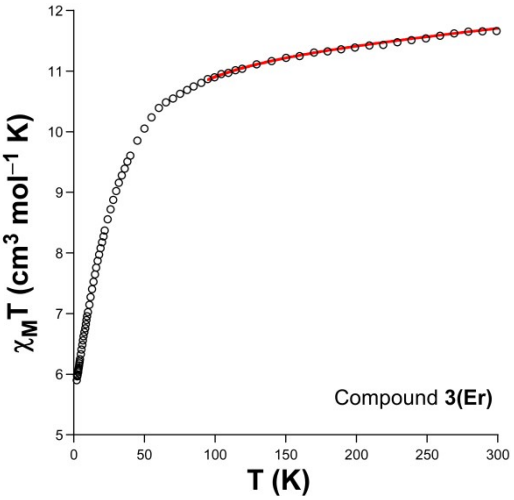

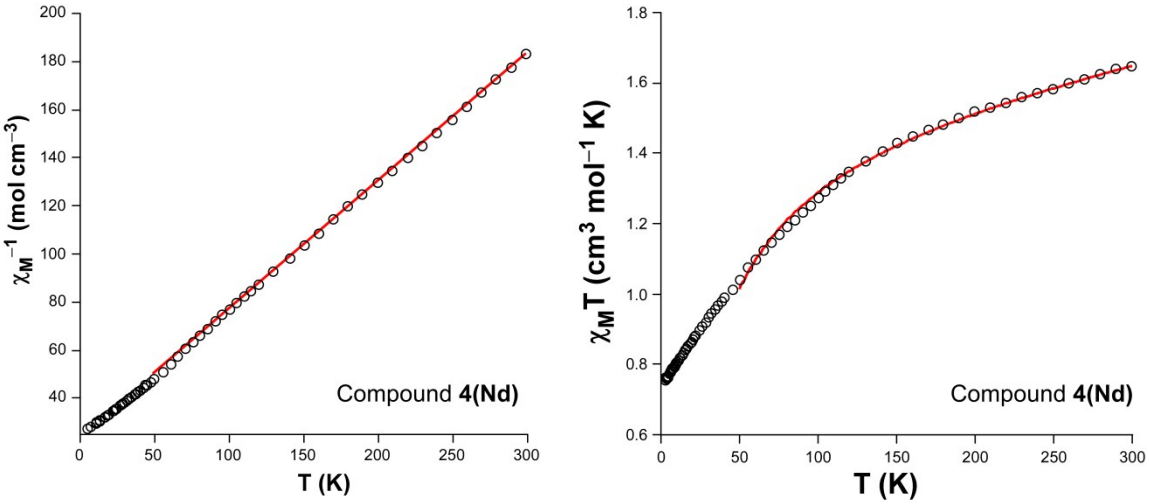

Figure S7. χ_M^{-1} vs T and $\chi_M T$ vs T plots of compounds **1**–**4** showing best theoretical fitting (red line).

Photoluminescence properties of compounds 1-4

Table S7. Characteristic intense emission peaks/bands of each rare metal studied.

	λ_{ex} /λ_{em}	Assig.
Dy^{3+}	480/575	$^4F_{9/2}\rightarrow{}^6H_{15/2}$
Tb^{3+}	485/ **548**	$^5D_4\rightarrow{}^7F_5$
Yb^{3+}	**975**/1050	$^2F_{5/2}\rightarrow{}^2F_{7/2}$
Nd^{3+}	900/**1060**	$^4F_{3/2}\rightarrow{}^4I_{11/2}$

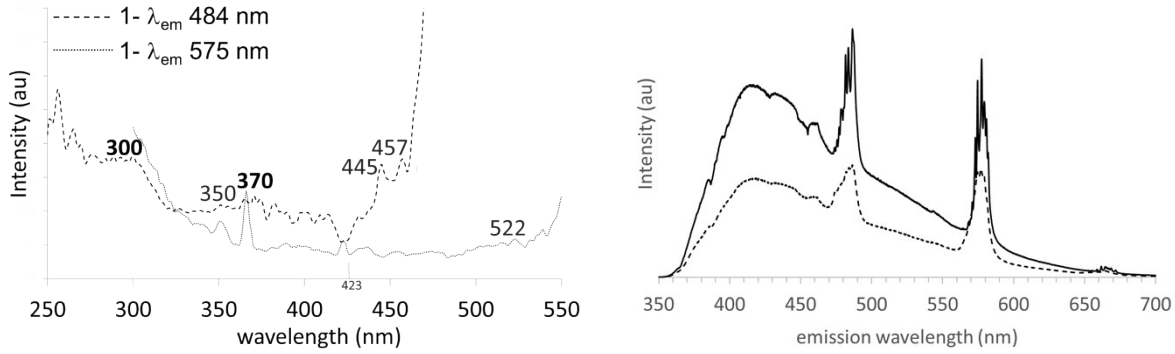

Figure S8. Left: Room temperature solid state excitation spectra of **1**, monitored at λem=484nm (dashed line) and λem=575 nm (solid line). The excitation spectra revealed, among others, a wide maximum around 300 nm and a narrow maximum around 370 nm, signals assigned to π← π* transitions inside the ligand. Right: Low temperature (50K, dashed line) and room temperature (solid line) solid state emission spectra of **1** upon sample excitation at λex= 325 nm.

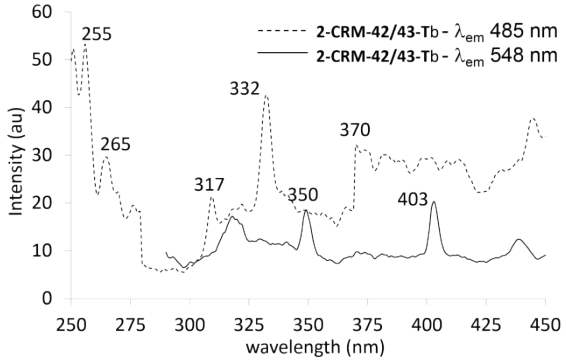

Figure S9. Room temperature solid state excitation spectra of 2, monitored around the metal´s (Tb^{3+}) more intense emission lines, λem=485nm (dashed line) and λem=548 nm (solid line), assigned to $^5D_4\rightarrow{}^7F_J$ transitions.

Moreover, for a complete knowledge of our complexes with Caco-2 cells, it has been investigated all compounds with normal cells. Caco-2 cells, upon reaching confluence, form a monolayer of polarized cells, presenting a structure of brush border on the apical surface with tight junctions. This brush border is comparable to the one observed in healthy human small-intestinal tissue, expressing also the same hydrolases, nutrient transporters, bacterial receptors, and other proteins present in enterocytes-like differentiated cells.

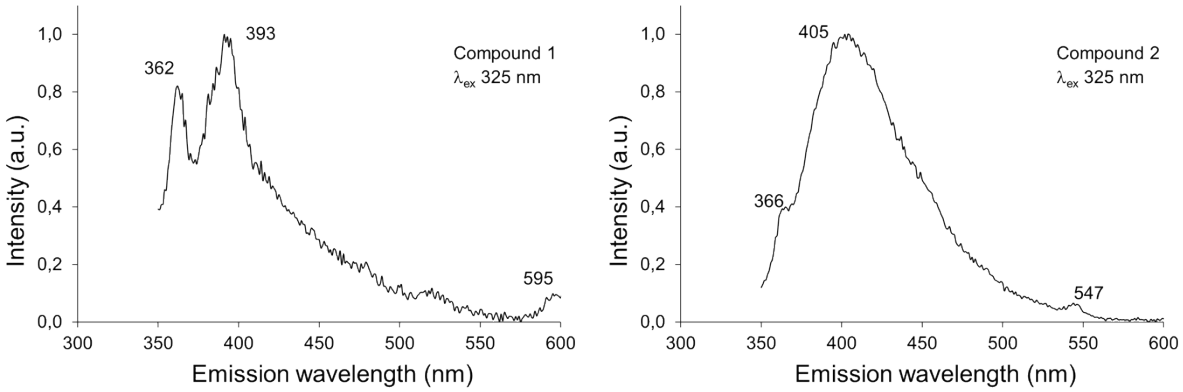

Figure S10. Room temperature emission spectra of water solutions of **1** (left) and **2** (right) (λ_{ex}=325nm). The emission spectra revealed that luminescent processes in 1 or 2, involving the central metal cations, are largely quenched in solution; in this respect, a weak band is observed centered at ca. 595 nm in **1** and ca. 547 nm in **2**, which are negligible compared to the ligand derived emission bands observed at shorter wavelengths.